Conformational Equilibria of TADDOL-s in Solution Investigated by Vibrational Circular Dichroism

ARTICLE *in* CHIRALITY · JANUARY 2010

Impact Factor: 1.89 · DOI: 10.1002/chir.20829 · Source: PubMed

9 AUTHORS, INCLUDING:

Dragos Gherase
The Scripps Research Institute
13 PUBLICATIONS **60** CITATIONS
SEE PROFILE

Florina Teodorescu
Romanian Academy
13 PUBLICATIONS **35** CITATIONS
SEE PROFILE

Nicolas Daugey
French National Centre for Scientific Research
21 PUBLICATIONS **316** CITATIONS
SEE PROFILE

Daniel Liotard
Université Bordeaux 1
85 PUBLICATIONS **1,039** CITATIONS
SEE PROFILE

Conformational Equilibria of TADDOL-s in Solution Investigated by Vibrational Circular Dichroism

CORNELIA UNCUTA,[1]* EMERIC BARTHA,[1] DRAGOS GHERASE,[1] FLORINA TEODORESCU,[1] CONSTANTIN DRAGHICI,[1] DOMINIQUE CAVAGNAT,[2] NICOLAS DAUGEY,[2] DANIEL LIOTARD,[2] AND THIERRY BUFFETEAU[2]*

[1]*Centre for Organic Chemistry "Costin D. Nenitescu", Romanian Academy, Bucharest 060023, Romania*
[2]*Institut des Sciences Moléculaires, Université de Bordeaux 1 (CNRS UMR5255), Talence Cedex 33405, France*

Contribution to the CD ISBC 2009 Special Issue

ABSTRACT Six enantiomeric pairs of TADDOL-s gathered in two series with either methyl (series **A**) or phenyl (series **B**) substituent in 2-position of the dioxolane ring were studied by vibrational circular dichroism (VCD). Experimental IR and VCD spectra associated with density functional theory (DFT) calculations showed that the two series exhibit quite different conformations in solution. In series **A**, the conformer with *anti* C—O bonds and stabilized by intramolecular OH···OH hydrogen bonding prevails, whereas in series **B** the conformer with *gauche* C—O bonds and intramolecular OH···π hydrogen bonding is favored. The shape and sign of the VCD bands in the O—H stretching region revealing the nature of the intramolecular hydrogen bonding were clearly identified. Polarimetric measurements showed that, within the same absolute configuration, compounds in series **A** and in series **B** have opposite signs of optical rotation. *Chirality 22:E115–E122, 2010.*

KEY WORDS: vibrational circular dichroism; DFT calculations; conformational analysis; TADDOL

INTRODUCTION

TADDOL-s are a class of compounds with many applications in the field of asymmetric synthesis and enantiomeric resolution of racemates.[1,2] The key issue in their ability and versatility as chiral additives resides in a conformational preference based on intramolecular hydrogen bonding. A direct proof of this preference comes from crystallographic data on TADDOL-s and their inclusion compounds with hydrogen bond donors, indicating a common seven-membered ring core shaped by an intramolecular OH···OH hydrogen bonding (such as in **1A**, Scheme 1). Only a few exceptions to this rule have been observed.[3–6] The most notable is the solvent-free hexaphenyl-TADDOL, stabilized in a completely different conformation involving two OH···π bydrogen bonding (**1B**, Scheme 1). The conformational change leads to a substantially different arrangement of the aromatic ring blades in these propeller-like molecules.

Should the "current" (A)/"uncurrent" (B) conformational dichotomy be preserved in solution, a significant modulation in the chiroptical properties is to be expected. The purpose of the present article is to study systematically the conformational equilibrium of TADDOL-s in solution through vibrational circular dichroism (VCD). Indeed, VCD seems the ideal tool for such an investigation, being a well established method for determination of absolute configuration as well as solution conformation of chiral molecules.[7,8] The method entails comparison of experimental VCD spectrum with spectra calculated at the density functional theory (DFT) level for conformers of specified absolute configuration.[9]

The TADDOL-s and their simple derivatives with (*R*,*R*) configuration are levorotatory in chloroform, but a few derivatives exhibiting uncurrent conformation in solid state were reported to be dextrorotatory in the same solvent.[4,5] This sign reversal under conformational change within the same configuration has also been checked by polarimetric measurements.

MATERIALS AND METHODS

Materials

Melting points were determined on Boetius hot stage and are uncorrected. The elemental analyses were performed with a ECS 4010 COSTECH instrument. The NMR

Additional Supporting Information may be found in the online version of this article.

Contract grant sponsors: CNRS (Chemistry Department), Région Aquitaine
Contract grant sponsor: Romanian Ministry of Education (CEx); Contract grant number: 60/2006
Contract grant sponsor: UEFISCSU; Contract grant number: 53/2007

*Correspondence to: Dr. T. Buffeteau, Institut des Sciences Moléculaires, Université de Bordeaux 1 (CNRS UMR5255), 351 cours de la Libération, 33405 Talence Cedex, France. E-mail: t.buffeteau@ism.u-bordeaux1.fr or Dr. C. Uncuta, Centre for Organic Chemistry "Costin D. Nenitescu", Romanian Academy, 202B Spl. Independentei CP 35-108, Bucharest 060023, Romania.
E-mail: cornelia.uncuta@yahoo.com.

Received for publication 8 October 2009; Accepted 8 December 2009
DOI: 10.1002/chir.20829
Published online 16 March 2010 in Wiley Online Library (wileyonlinelibrary.com).

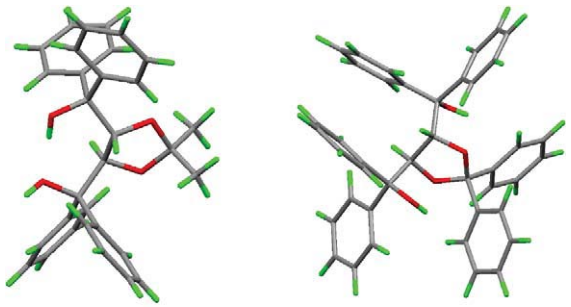

Scheme 1. "Current" **A** and "uncurrent" **B** conformation of TADDOLs as determined by X-ray diffraction in monocrystal.

spectra were recorded with Varian Gemini 300 BB instrument, operating at 300 MHz for ^{1}H and at 75 MHz for ^{13}C. The chemical shifts (δ) values are given in ppm from internal TMS, the coupling constants *J* are in Hz. Analytical TLC was performed with silica gel F_{254} (Merck) on aluminum strips (10 cm length). For column chromatography, silica gel 60 (Merck) was used. The starting optically active reagent was L-tartaric acid for (*R*,*R*)-TADDOL-s and (−) diethyl D-tartrate (Fluka) for (*S*,*S*)-TADDOL-s. Tetrahydrofuran (THF) freshly distilled from lithium aluminum hydride was used in the Grignard reaction. The elution solvents for chromatography are abbreviated as follows: diethylether (EE), benzene (B), petroleum ether (PE) with boiling range 40–67°C. The measurements of optical rotation were performed with a 341 Perkin Elmer polarimeter using a 1 cm path length glass cell. Concentration of TADDOL-s was 1g/100 ml in chloroform (pro analysi grade from Merck) solution.

The following TADDOL-s have already been described and were prepared according to literature procedure: (*R*,*R*)-**1A** and (*S*,*S*)-**1A**,[10] (*R*,*R*)-**2A**[11] and (*S*,*S*)-**2A**,[12] (*R*,*R*)-**3A**,[12] and (*S*,*S*)-**3A**,[13] (*R*,*R*)-**1B**,[3] (*R*,*R*)-**3B** and (*S*,*S*)-**3B**.[14]

(4*S*,5*S*)-α,α,α′,α′-2,2-Hexaphenyl-4,5-dimethanol-1,3-dioxolane, (*S*,*S*)-**1B** was prepared as its (*R*,*R*) enantiomer.[3] For purification, precipitation of the clathrate with ethanol was performed, followed by repeated azeotropic distillation with benzene. The solvent-free product was a colorless solid, which started softening on heating at 95–100°C.

(4*R*,5*R*)-2,2-Diphenyl-α,α,α′,α′-tetra(naphth-2-yl)1,3-dioxolane-4,5-dimethanol, (*R*,*R*)-**2B**: to the Grignard reagent[11] prepared from magnesium (1.82 g, 75 at. equiv) and 2-bromo-naphtalene (15.63 g, 75.5 mmol) in THF (30 ml) was added a solution of (4*R*,5*R*)-2,2-diphenyl-4,5-dimethoxycarbonyl-1,3-dioxolane[3] (4.97 g, 14.5 mmol) in THF (30 ml), keeping the internal temperature below 20°C (external cooling). The mixture was stirred overnight at room temperature then heated at reflux for 2 h. After cooling, water (100 ml) was added under vigorous stirring. The reaction mixture was filtered on a large surface Buchner funnel, the solid was washed with diethylether and the organic layer was separated. The aqueous layer was further extracted with ether, the combined organic layers washed with brine and dried over sodium sulfate. Evaporation of the solvent gave an yellow foam (11.8 g). The crude product was purified by repeated column chromatography on silica gel. First, elution was performed with EE/EP gradient mixtures, starting from 1:20 ratio and collecting the fraction eluted with 1:1 ratio of solvents. This fraction was subjected to the second column chromatography, eluting with B/PE mixtures, starting from 1:5 ratio and collecting the main fraction at 1:1 ratio. Evaporation of the solvent gave 2.69 g (23.5% yield) of analytically pure (*R*,*R*)-**2B**.

$$R_f = 0.47(\text{EE/EP } 1:1), R_f = 0.50(\text{B})$$

^{1}H-NMR($CDCl_3$): 2.34 (2H, s, OH), 6.07 (2H, s), 6.08 (2H, d, J = 8.8 Hz), 6.31 (2H, dd, J = 8.8 Hz, J = 1.6 Hz), 7.30–7.23 (6H, m), 7.30–7.39 (6H, m), 7.45–7.57 (10H, m), 7.65–7.68 (2H, m), 7.72 (2H, d, J = 8.8 Hz), 7.80 (2H, dd, J = 7.4 Hz, J = 1.6 Hz), 7.99 (2H, d, J = 8 Hz),8.05 (2H, d, J = 1.6 Hz), 8.30 (2Hd,J, 1.6 Hz).

^{13}C-NMR ($CDCl_3$): 80.6, 84.0, 113.2, 123.7, 124.2, 125.1, 125.8, 126.0, 126.2, 126.3, 127.5, 127.6, 127.8, 128.1, 128.3, 128.5, 128.8, 129.1, 132.1, 132.7, 133.0, 133.2, 139.0, 143.6, 145.1.

IR and VCD Measurements

The infrared (IR) and VCD spectra were recorded with a ThermoNicolet Nexus 670 FTIR spectrometer equipped with a VCD optical bench.[15] In this optical bench, the light beam was focused on the sample by a BaF_2 lens (191-mm focal length), passing an optical filter (depending on the studied spectral range), a BaF_2 wire grid polarizer (Specac), and a ZnSe photoelastic modulator (Hinds Instruments, Type II/ZS50). The light was then focused by a ZnSe lens (38.1-mm focal length) onto a 1 × 1 mm^2 HgCdTe (ThermoNicolet, MCTA* E6032) detector. Absorption and VCD spectra were recorded at a resolution of 4 cm^{-1} (8 cm^{-1} for experiments in the OH/CH stretching region), by coadding 50 scans and 36,000 scans (12 h acquisition time), respectively. Samples were held in a variable path length cell with BaF_2 windows. IR and VCD spectra of the two enantiomers of **1A**, **2A**, **3A**, **1B**, **2B**, and **3B** were measured in $CDCl_3$ solvent at a concentration of 0.08 M and at a path length of 250 μm. Baseline corrections of the VCD spectra were performed by subtracting the two opposite-enantiomer VCD spectra of **1A**, **2A**, **3A**, **1B**, **2B**, and **3B** (recorded under the same experimental conditions) with division by two. In all the experiments, the photoelastic modulator was adjusted for a maximum efficiency at 1400 cm^{-1} (3400 cm^{-1} for experiments in the OH/CH stretching region). Calculations were done with the standard ThermoNicolet software, using Happ and Genzel apodization, de-Haseth phase-correction and a zero-filling factor of one. Calibration spectra were recorded using a birefringent plate (CdSe) and a second BaF_2 wire grid polarizer, following the experimental procedure previously published.[16] Finally, in the presented absorption spectra, the solvent absorption was subtracted out.

DFT Calculations

The calculation of the IR and VCD spectra began with a thorough analysis of the conformational freedom of the

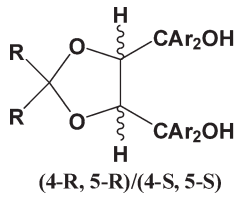

Ar\R	Me	Ph
Ph	1A	1B
2-Npht	2A	2B
1-Npht	3A	3B

Scheme 2. Structure and numbering of TADDOL-s.

TADDOL molecules. This involved exploring the entire conformational energy surface of the molecules and carrying out semiempirical RM1[17] calculations with the simulated annealing technique,[18] as both implemented in the package Ampac,[19] of the relative energies of conformers found in the various local minima of this surface. The search for energetic minima was performed in two stages: (i) a nonlocal seek focused on main torsional angles and (ii) a local energetic relaxation of the whole degrees of freedom, for each of the minima collected at stage (i). All conformers within roughly 8 kcal/mole of the lowest energy conformer were kept for further DFT calculations.

The geometry optimizations, vibrational frequencies, absorption, and VCD intensities were calculated by Gaussian 03 program[20] on a SGI Altix XE 1300 (with four processors) of the Pôle Modélisation of the Institut des Sciences Moléculaires (University Bordeaux I). Calculations of the optimized geometry of twelve conformers of (4*S*,5*S*)-**1A** and twenty conformers of (4*S*,5*S*)-**1B** were performed at the density functional theory level using B3PW91 functional and 6-31G* basis set. Vibrational frequencies, IR, and VCD intensities were calculated at the same level of theory, utilizing the magnetic field perturbation method with gauge-invariant atomic orbitals.[21] The spectra were calculated for the isolated molecule in vacuo and for TADDOL in solution, using the polarizable continuum model (PCM).[22] For comparison to experiment, the calculated frequencies were scaled by 0.968 (0.954 for calculations in the OH/CH stretching region) and the calculated intensities were converted to Lorentzian bands with a half-width of 7 cm^{-1} (15 cm^{-1} for calculations in the OH/CH stretching region). A half-width of 50 cm^{-1} has been used for the stretching vibration of hydroxyl groups involved in OH···OH hydrogen bonds.

RESULTS AND DISCUSSION

The Design of TADDOL-s

Scheme 2 presents the structure and numbering of the investigated TADDOL-s, differentiated by the nature of the aryl groups (phenyl, 2-naphthyl, 1-naphthyl) and paired according to the substituent in the dioxolane ring into series **A** (R = Me) and series **B** (R = Ph). The reason for the **A**/**B** pairing resides in the expectation of current conformation occurring in series **A** and uncurrent conformation in series **B**. For VCD measurements, both (4*R*, 5*R*) and (4*S*, 5*S*) enantiomers have been prepared, raising to 12 the total number of the investigated compounds.

Polarimetric Measurements

Table 1 displays the specific rotation values $[\alpha]_D^{25}$ of the TADDOL-s, measured in chloroform solution. In each **A**/**B** pair of the same absolute configuration, an inversion in the rotation sign is observed. This results also agrees with previous reports,[4,5] meaning that (*R*,*R*)-TADDOL-s with conformation **A** in solution are levorotatory, while those with conformation **B** are dextrorotatory. Although such empirical correlations are of limited use, the systematic character of the present experimental data emphasizes the conformational effect on chiroptical properties in the class of TADDOL-s.

Experimental IR and VCD Spectra

The IR spectra of (4*S*,5*S*) enantiomer of **1A**, **2A**, **3A**, **1B**, **2B** and **3B** in $CDCl_3$ solution in the OH/CH stretching region and in the mid-IR spectral region are shown in Figures 1a and 1b, respectively. Compounds of series **A** and **B** exhibit different IR spectra in the OH stretching region. The IR spectra of **1A** and **3A** in $CDCl_3$ solution show a band at 3582 cm^{-1} assigned to the stretching vibration of "free" hydroxyl groups and a broad band at 3372 cm^{-1} assigned to the stretching vibration of hydroxyl groups which formed intra- and/or intermolecular hydrogen bonds. These bands are located at lower wavenumbers for the compound **2A** (3576 cm^{-1} and 3351 cm^{-1}, respectively). On the other hand, the IR spectra of **1B** and **3B** in $CDCl_3$ solution show a sharp band at 3548 cm^{-1} assigned to the stretching vibration of hydroxyl groups involved in OH···π hydrogen bonds. This band is located at higher wavenumbers (3556 cm^{-1}) for compound **2B**. It is noteworthy that a very weak broad band at 3385 cm^{-1} is also observed in the IR spectrum of **1B**. The different behavior observed in the OH stretching region for the two series may be attributed to a conformational change of TADDOL-s in solution. The IR spectra in the aromatic and aliphatic CH stretching vibrations (spectral range between 3200 and 2800 cm^{-1}) are strongly dependent on the nature of the aryl groups (phenyl, 2-naphthyl, 1-naphthyl) and on the substituent in the dioxolane ring (methyl or phenyl). However, the two series can be differentiated considering the C—H stretching vibrations of the two asymmetric carbons. Indeed, the *C—H stretching vibrations are located at 2898 cm^{-1} for the series **A** and at 2967 cm^{-1} for the series **B**. Finally, it is difficult to extract information on conformation of TADDOL-s in the mid-IR spectral region since the main bands observed in the IR spectra are essentially associated to the aryl groups and to the substituent (methyl or phenyl). The IR spectra in this spectral range are specific of each compound and no tendency can be drawn for the two series.

TABLE 1. Specific rotation values $[\alpha]_D^{25}$ of TADDOL-s

	1A	1B	2A	2B	3A	3B
(*R*,*R*)	−65[a]	+178[b]	−75[c]	+303	−162	+290[d]
(*S*,*S*)	+64[e]	−173	+75[f]	−302	+182	−290

Literature $[\alpha]_D^{25}$: (a) −65.1,[12]; (b) +60.7,[12]; (c) +177.1,[23]; (d) −115.4 (ethyl acetate),[12]; (e) −114.1 (ethyl acetate),[12]; (f) +293,[14].

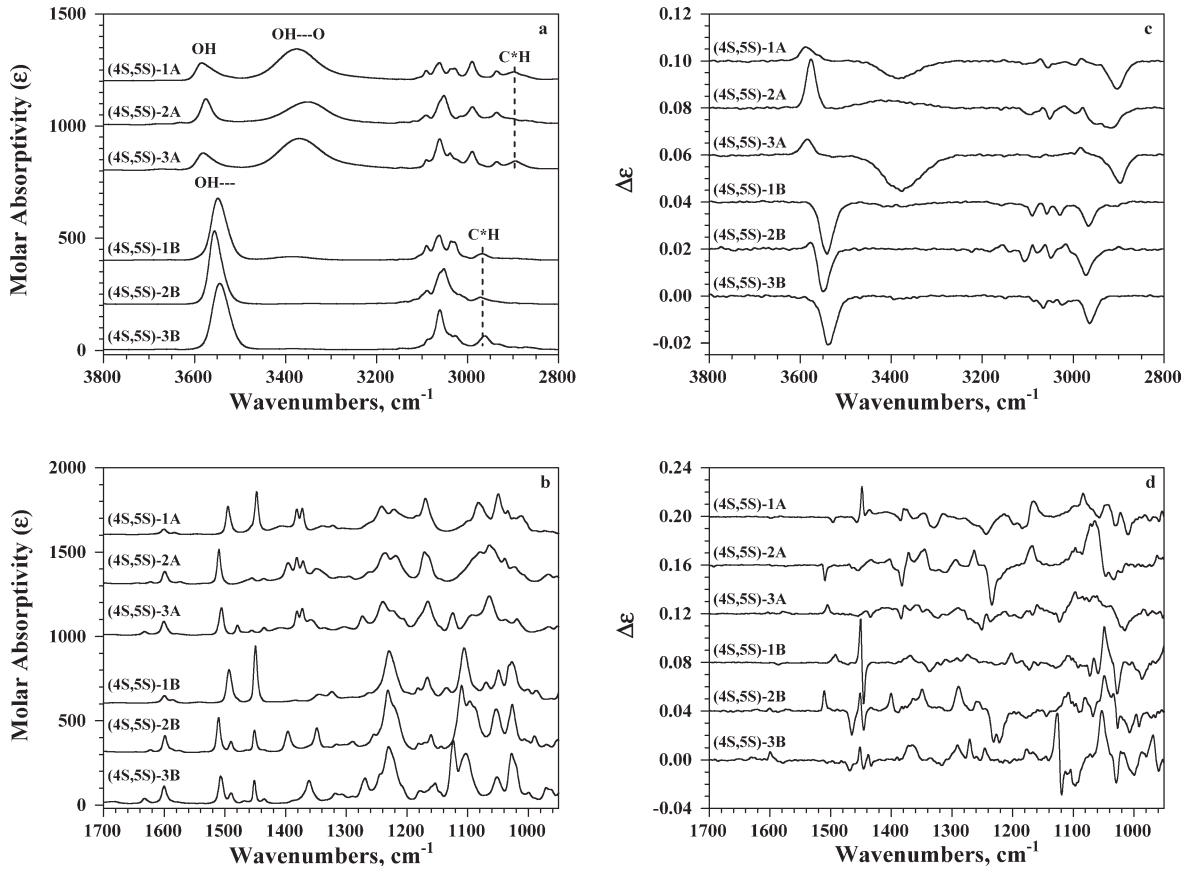

Fig. 1. (**a**,**b**) IR and (**c**,**d**) VCD spectra of **1A**, **2A**, **3A**, **1B**, **2B**, and **3B** in $CDCl_3$ solution (a,c) in the OH/CH stretching region and (b,d) in the mid-IR spectral region.

The VCD spectra of (4*S*,5*S*) enantiomer of **1A**, **2A**, **3A**, **1B**, **2B** and **3B** in $CDCl_3$ solution in the OH/CH stretching region and in the mid-IR spectral region are shown in Figures 1c and 1d, respectively. Figure 1c reveals strong VCD bands associated with hydroxyl and *CH groups. The *C—H stretching vibrations give rise to a negative band located at 2898 cm^{-1} for the series **A** and at 2966 cm^{-1} for the series **B**. The sign of this band is independent on the conformation of the molecule and may be related to the absolute configuration of TADDOL-s: a negative band is associated with the (4*S*,5*S*) enantiomer whereas a positive band is associated with the (4*R*,5*R*) enantiomer. VCD spectra exhibit different behavior in the OH stretching region for the two series. The O—H stretching vibrations of the free hydroxyl groups give rise to a positive band located at 3585 cm^{-1} for compounds **1A** and **3A** and at 3576 cm^{-1} for **2A**. The stretching vibration of hydroxyl groups which formed intra- and/or intermolecular hydrogen bonds give rise to a negative broad band located at 3380 cm^{-1} for compounds **1A** and **3A** and to a positive very weak broad band at 3410 cm^{-1} for **2A**. The width and the sign of this band come certainly from the more or less large distribution of OH···OH hydrogen bonds. The VCD spectra of **1B**, **2B**, and **3B** are very similar in the OH stretching region and show a negative sharp band at 3540 cm^{-1} characteristic to the OH···π hydrogen bonds. A negative very weak broad band at 3380 cm^{-1} is also observed in the VCD spectrum of **1B**, suggesting the presence of a small amount of OH···OH hydrogen bonds. On the other hand, the two series cannot be differentiated from the VCD spectra presented in Figure 1d in the mid-IR spectral region.

Conformational Analysis of 1A and 1B

The conformational analysis of **1A** and **1B** was carried out initially using semiempirical RM1 calculations with the simulated annealing technique. Twelve conformers for **1A** and twenty conformers for **1B** with energies within 8 kcal/mol of the lowest energy conformer, resulted. Subsequently, the twelve (twenty) RM1 conformations of **1A** (**1B**) were optimized using DFT at the B3PW91/6-31G* level. Calculations were performed for the isolated molecule in vacuo and for TADDOL in solution, using the polarizable continuum model (PCM). Harmonic vibrational frequencies have been calculated at the same level to confirm that all structures are stable conformations and to enable free energies to be calculated. The electronic and Gibbs energies calculated using PCM model, room-temperature populations determined from Gibbs energies and structural parameters are listed in Table 2.

TABLE 2. Conformations, energies and structural parameters of 1A and 1B

Conf.	Energy[a] Electronic	Energy[a] Gibbs	ΔG[b] (kJ/mol)	P[c] (%)	Structural parameters D_1[d] (°)	D_2[e] (°)	D_3[f] (Å)
Compound 1A							
A1	−1499.676912	−1499.198785	0	37.2	175.8	167.5	2.71
A2	−1499.676964	−1499.198750	0.09	36.0	174.8	172.9	2.70
A3	−1499.676223	−1499.198379	1.06	24.0	−175.1	−164.0	2.70
A4	−1499.673121	−1499.196388	6.29	2.8	−58.9	162.7	4.20
Compound 1B							
B1	−1882.994012	−1882.421787	0	64.8	−66.6	−66.6	5.07
B2	−1882.992881	−1882.420382	3.7	14.3	−66.3	163.7	4.20
B3	−1882.993762	−1882.420259	4.0	12.5	166.5	176.4	2.73
B4	−1882.992183	−1882.419396	6.3	4.9	−66.8	−170.7	4.41
B5	−1882.992907	−1882.419073	7.1	3.5	171.8	168.5	2.73

[a]In hartrees.
[b]Relative Gibbs energy difference.
[c]Population based on Gibbs energies.
[d]O3−*C2−C−O dihedral angle (see numbering in Supporting Information).
[e]O6−*C1−C−O dihedral angle (see numbering in Supporting Information).
[f]Distance between the two oxygen atoms of hydroxyl groups.

Based on the ab initio predicted Gibbs energies, it can be concluded that **1A** exists predominantly in three main conformations A1, A2, and A3. These three conformations show an antiperiplanar relationship between the endocyclic and exocyclic C—O bonds, as revealed by the D_1 and D_2 dihedral angles close to ±170°. The D_3 distance between the two oxygen atoms of hydroxyl groups (2.70 Å) and the O···H distance of about 1.76 Å indicate that these conformers are stabilized by OH···OH intramolecular hydrogen bond. The principal variations in the structures of conformations A1, A2, and A3 are associated with very slight rotation around the two *C—C bonds as shown in the Supporting Information. A fourth conformation, A4, has been calculated with a very low contribution (<3%). In this conformation, one O—*C—C—O dihedral angle is about 163° (*trans* conformation) but the second dihedral angle is close to 60° (gauche conformation). This conformation is stabilized by interaction of one hydroxyl group with a phenyl group (distance H···Ph of 3.07 Å).

Concerning **1B**, it clearly appears that conformation B1 with synclinal relationship between the endocyclic and exocyclic C—O bonds is of lowest energy and represents 65% of the different conformers at room temperature. This contribution is higher (about 75%) when DFT calculations were performed for the isolated molecule in vacuo. As shown in the Supporting Information, the structure of this conformer is symmetric (pseudo C_2-symmetry) with the D_1 and D_2 dihedral angles equal to −66.6° (gauche conformation). This conformation is stabilized by OH···π interaction with the phenyl subtituents (distance H···Ph of 3.09 Å). Four other conformers present non-negligible populations: conformers B2 and B4 with a trans and gauche conformations of the O—*C—C—O segments (similar to conformer A4) and conformers B3 and B5 with trans conformation of the two O—*C—C—O segments stabilized by OH···OH intramolecular hydrogen bond. These two last conformers represent 16% (8.7% for the isolated molecule in vacuo) of the different conformers at room temperature.

Calculated IR and VCD Spectra of 1A

The frequencies, dipolar strengths and rotational strengths of the 3N-6 (i.e., 189) vibrations, calculated in vacuo and in $CDCl_3$ using the PCM model at the B3PW91/6-31* level for individual conformers A1, A2, A3, and A4 are given in the Supporting Information. The population-weighted IR and VCD spectra calculated in vacuo [labeled Predicted (4*S*,5*S*)-1A] and in $CDCl_3$ [labeled Predicted (4*S*,5*S*)-1A (PCM)] are shown in Figure 2 and compared to the corresponding experimental IR and VCD spectra of **1A** in 0.08 M $CDCl_3$ solution. IR spectrum calculated using the PCM model exhibits slightly higher intensity than that calculated in vacuo but the overall shape of the spectra is similar. The frequencies are not modified for most of the bands, except for the stretching and bending vibrations involving hydroxyl groups.

Figures 2a and 2b show that the predicted IR spectra are in relatively good agreement with the experimental spectrum of **1A**, except for the bands associated with CH stretching vibrations of aromatic groups between 3100 and 3000 cm^{-1}. This discrepancy comes from the electrical anharmonicity of the CH stretching modes that is not considered in the Gaussian package and the too large half-width used (15 cm^{-1}) for these vibrations when calculated intensities are converted to Lorentzian bands. Similarly, some bands associated with aromatic groups in the mid-IR (at 1495, 1447, 1170, and 1050 cm^{-1}) exhibit narrow shape than those calculated with half-width of 7 cm^{-1}. Nevertheless, the two bands at 3583 and 3375 cm^{-1} are perfectly reproduced in the predicted spectra and confirm their assignment to the O—H stretching vibrations of the free and bonded hydroxyl groups, respectively.

Figures 2c and 2d show that the predicted VCD spectra reproduces fairly well the intensity and the sign of the

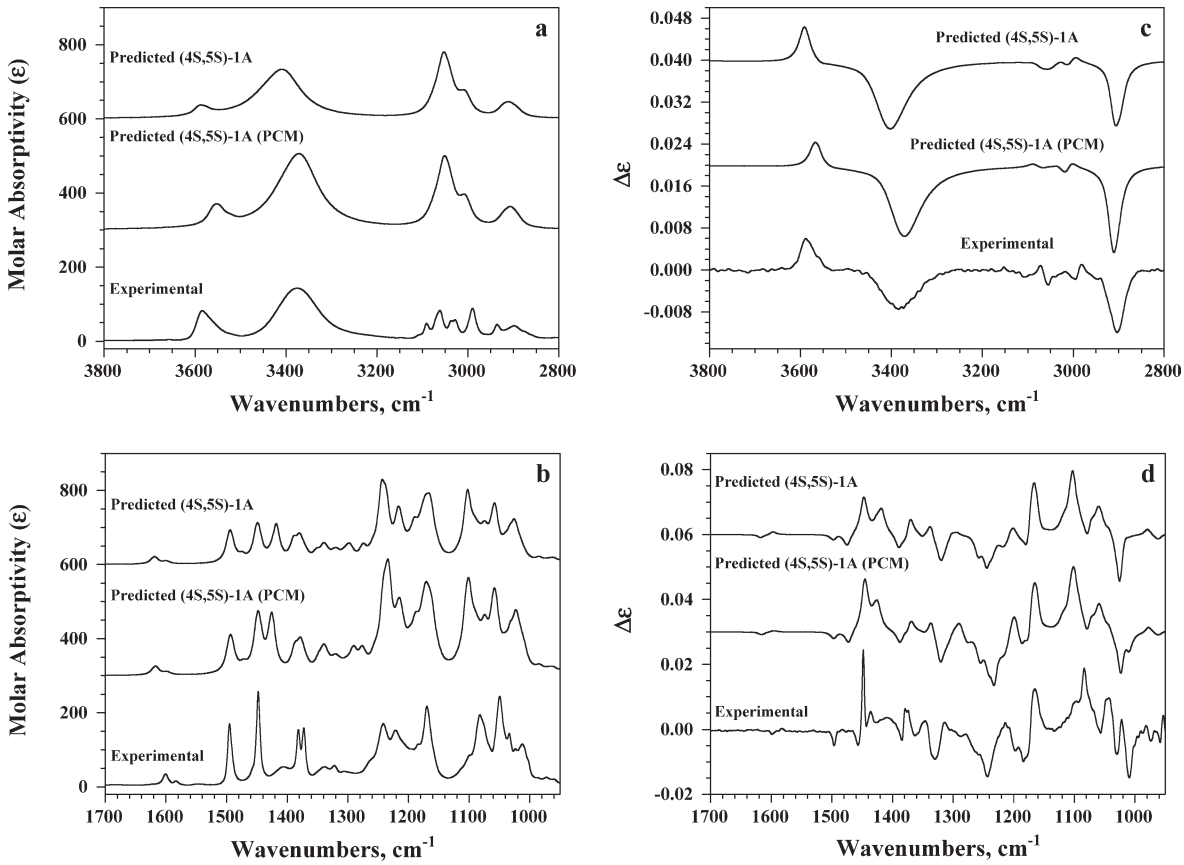

Fig. 2. Comparison of experimental (**a**,**b**) IR and (**c**,**d**) VCD spectra (bottom) of **1A** in $CDCl_3$ solvent with predicted (population weighted) IR and VCD spectra calculated using the PCM model (medium) and in vacuo (top) at the B3PW91/6-31G* level in (a,c) the 3800–2800 cm^{-1} and (b,d) the 1700–950 cm^{-1} regions.

bands observed in the experimental spectrum, confirming the (4*S*,5*S*) configuration of the molecule (+)-**1A** and allowing the definitive determination of its conformation (antiperiplanar relationship between the endocyclic and exocyclic C—O bonds). The agreement between predicted and experimental spectra is particularly excellent in the OH/CH stretching region (Fig. 2c) even for the CH stretching vibrations of the aromatic groups.

Calculated IR and VCD Spectra of 1B

The frequencies, dipolar strengths and rotational strengths of the 3N-6 (i.e., 231) vibrations, calculated in vacuo and in $CDCl_3$ using the PCM model at the B3PW91/6-31* level for individual conformers B1, B2, B3, B4, and B5 are given in the Supporting Information. The population-weighted IR and VCD spectra calculated in vacuo [labeled Predicted (4*S*,5*S*)-1B] and in $CDCl_3$ [labeled Predicted (4*S*,5*S*)-1B (PCM)] are shown in Figure 3 and compared to the corresponding experimental IR and VCD spectra of **1B** in 0.08 M $CDCl_3$ solution.

As shown in Figures 3a and 3b, the predicted IR spectra are in very good agreement with the experimental spectrum of **1B**, except for the CH stretching vibration of the aromatic groups. The sharp band at 3548 cm^{-1} assigned to the stretching vibration of hydroxyl groups involved in OH···π hydrogen bonds are perfectly reproduced as well as the broad band at 3385 cm^{-1} assigned to the stretching vibration of hydroxyl groups forming intramolecular OH···OH hydrogen bonds. The intensity of this last band is slightly overestimated in the predicted spectrum calculated using the PCM model whereas it is correct for calculation in vacuo.

The comparison of the predicted VCD and experimental spectra confirms the (4*S*,5*S*) configuration of the molecule (−)-**1B** and shows that the synclinal relationship between the endocyclic and exocyclic C—O bonds is the predominant conformation of **1B**. This conformation is stabilized by OH···π interaction with the two phenyl subtituents in the dioxolanic ring. The presence of the broad band at 3385 cm^{-1} in the experimental and predicted VCD spectra reveals also the contribution of a small amount of conformers stabilized by OH···OH intramolecular hydrogen bonds.

DISCUSSION

Two main conformations of TADDOL-s have been found depending only on the substituent R in the dioxolane ring, as shown in Scheme 3. The nature of the aryl groups (phenyl, 2-naphthyl and 1-naphthyl) does not appreciably change the preferential conformation observed for each series **A** and **B**.

The conformational flexibility of TADDOL-s in solution may be explained by the *anti/gauche* equilibrium involving the two O—C*—C(Ar_2)O moieties. The *anti* conformation

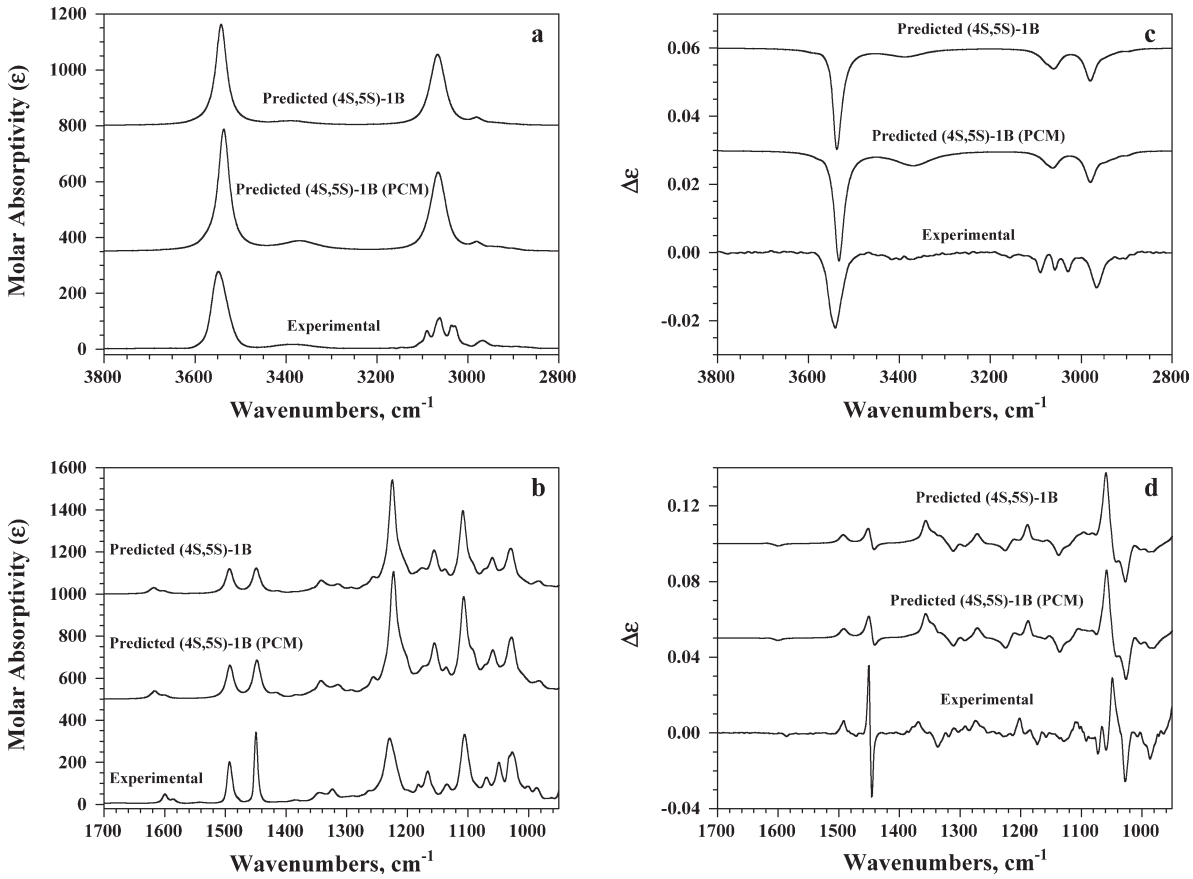

Fig. 3. Comparison of experimental (**a**,**b**) IR and (**c**,**d**) spectra (bottom) of **1B** in $CDCl_3$ solvent with predicted (population weighted) IR and VCD spectra calculated using the PCM model (medium) and in vacuo (top) at the B3PW91/6-31G* level in (a,c) the 3800–2800 cm^{-1} and (b,d) the 1700–950 cm^{-1} regions.

is favored by the opposite position of the C—O bonds dipoles, while the *gauche* conformation by the maximal interaction between the best donor (lone pair n_O) and the best acceptor bond, σ^*_{CO} ("gauche effect").[24] The equilibrium mixture should consist of "anti, anti," "gauche, gauche," and "anti, gauche" conformers.

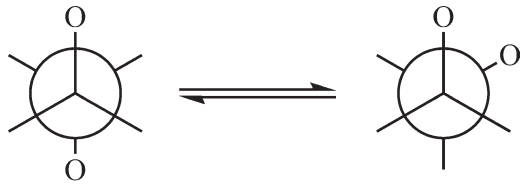

anti gauche

Further stabilizing interactions, such as intramolecular OH···OH in **1A** or OH···π hydrogen bondings in **1B**, shift the equilibrium towards prevalence of "anti, anti" or "gauche, gauche" conformer, respectively, as predicted by DFT calculations and fully substantiated by VCD results.

The DFT calculations indicated also a decrease in population of the "gauche, gauche" conformer B1 calculated with solvent contribution compared to the isolated molecule in vacuo (65% vs. 75%). This result might be explained by the solvent interacting with the lone pairs on oxygen and thereby interfering with the n–σ^* interactions, weakening the "gauche effect".

CONCLUSION

This article shows that modeling of infrared and vibrational circular dichroism spectra using density functional theory can be successfully performed to determine the

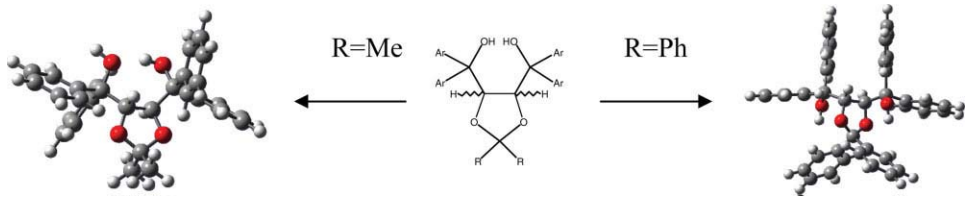

Scheme 3. Two main conformations of TADDOL-s. [Color figure can be viewed in the online issue, which is available at www.interscience.wiley. com.]

absolute configurations and conformations of TADDOL-s in solution. TADDOL-s with methyl substituents in the dioxolane ring exhibit an *anti* conformation of the endocyclic/exocyclic C—O bonds stabilized by intramolecular OH···OH hydrogen bonding. On the other hand, a *gauche* conformation of the two C—O bonds has been found for TADDOL-s with phenyl substituents in the dioxolane ring. This latter conformation is stabilized by OH···π hydrogen bonding.

ACKNOWLEDGMENTS

The authors acknowledge computational facilities provided by the Pôle Modélisation of the Institut des Sciences Moléculaires (University Bordeaux 1).

LITERATURE CITED

1. Seebach D, Beck AK, Heckel A. TADDOLs, their derivatives, and TADDOL analogs: versatile chiral auxiliaries. Angew Chem Int Ed 2001;40:92–138.
2. Pellisier H. Use of Taddols and their derivatives in asymmetric synthesis. Tetrahedron 2008;64:10279–10317.
3. Irurre J, Alonso-Alija C, Piniella JF, Alvarez-Larena A. Synthesis and structure of (4*R*,5*R*)-a,a,a′,a′-2,2-hexaphenyl-4,5-dimethanol-1,3-dioxolane. Tetrahedron: Asymmetry 1992;3:1591–1596.
4. Seebach D, Rheiner PB, Beck AK, Kuehnle FNM, Jaun B. Preparation and cationic rearrangements of ortho- and para-methoxy-TADDOLs. Polym J Chem 1994;68:2397–2413.
5. Seebach D, Pichota A, Beck AK, Pinkerton AB, Litz T, Karjalainen J, Gramlich V. Preparation of TADDOL derivatives for new applications. Org Lett 1999;1:55–58.
6. Seebach D, Beck AK, Hayakawa M, Jaeschke G, Kuhnle FNM, Nageli I, Pinkerton AB, Rheiner PB, Duthaler RO, Rothe PM, Weigand W, Wunsch R, Dick S, Nesper R, Worle M, Gramlich V. TADDOLs on their way to late transition metal complexes—synthesis and crystal structure of N- and S-containing TADDOL-derived compounds. Bull Soc Chim Fr 1997;134:315–331.
7. Freedman TB, Cao X, Dukor RK, Nafie LA. Absolute configuration determination of chiral molecules in the solution state using vibrational circular dichroism. Chirality 2003;15:743–758.
8. Buffeteau T, Cavagnat D, Bouchet A, Brotin T. Vibrational absorption and circular dichroism studies of (−)-camphanic acid. J Phys Chem A 2007;111:1045–1051.
9. Stephens PJ, Delvin FJ. Determination of the structure of chiral molecules using ab initio vibrational circular dichroism spectroscopy. Chirality 2000;12:172–179.
10. Toda F, Tanaka K. Design of a new chiral host compound, trans-4,5-bis(hydroxydiphenylmethyl)-2,2-dimethyl-1,3-dioxacyclopentane. An effective optical resolution of bicyclic enones through host-guest complex formation. Tetrahedron Lett 1988;29:551–554.
11. Beck AK, Gysi P, La Vecchia L, Seebach D. (4*R*,5*R*)-2,2-dimethyl-a,a,a′,a′-tetra(naphth-2-yl)-1,3-dioxolane-4,5-dimethanol from dimethyl tartrate and 2-naphthyl-magnesium bromide (1,3-dioxolane-4,5-dimethanol, 2,2-dimethyl-a,a,a′,a′-tetra-2-naphthalenyl-, (4*R*-trans)-). Org Synth 1999;76:12–22.
12. Beck AK, Bastani B, Plattner DA, Petter W, Seebach D, Braunschweiger H, Gysi P, La Vecchia L. Large-scale preparation of a,a,a′,a′-tetraaryl-1,3-dioxolane-4,5-dimethanol derivatives (TADDOLs), useful auxiliaries for enantioselective synthesis and their structure in the solid state. Chimia 1991;45:238–241.
13. Seebach D, Dahinden R, Marti RE, Beck AK, Plattner DA, Kuhnle FNM. On the Ti-TADDOLate-catalyzed diels-alder addition of 3-butenoyl-1,3-oxazolidin-2-one to cyclopentadiene. General features of Ti-BINOLate- and Ti-TADDOLate-mediated reactions. J Org Chem 1995; 60:1788–1799.
14. Cuenca A, Medio-Simon M, Aguilar GA, Weibel D, Beck AK, Seebach D. Highly enantioselective protonation of the 3,4-dihydro-2-methylnaphthalen-1(2H)-one Li-enolate by TADDOLs. Helv Chim Acta 2000; 83:3153–3162.
15. Buffeteau T, Lagugné-Labarthet F, Sourisseau C. Vibrational circular dichroism in general anisotropic thin solid films: Measurement and theoretical approach. Appl Spectrosc 2005;59:732–745.
16. Nafie LA, Vidrine DW. Double modulation fourier transform spectroscopy. In: Ferraro JR, Basile LJ, editors. Fourier transform infrared spectroscopy, Vol. 3. New York: Academic Press; 1982. pp. 83–123.
17. Rocha GB, Freire IO, Simas AM, Stewart JJP. RM1: A reparameterization of AM1 for H, C, N, O, P, S, F, Cl, Br, and I. J Comput Chem 2006; 27:1101–1111.
18. Bockisch F, Liotard D, Rayez JC, Duguay B. Simulated annealing to locate various stationary points in semiempirical methods. Int J Quantum Chem 1992;44:619–642.
19. Semichem. AMPAC-8. KS: Semichem, 2004.
20. Gaussian 03, revision B. 04.Frisch MJ, Trucks GW, Schlegel HB, Scuseria GE, Robb MA, Cheeseman JR, Montgomery JA Jr., Vreven T, Kudin KN, Burant JC, Millam JM, Iyengar SS, Tomasi J, Barone V, Mennucci B, Cossi M, Scalmani G, Rega N, Petersson GA, Naktasuji H, Hada M, Ehara M, Toyota K, Fukuda R, Hasegawa J, Ishida M, Nakajima T, Honda Y, Kitao O, Nakai H, Klene M, Li X, Knox JE, Hratchian HP, Cross JB, Adamo C, Jaramillo J, Gomperts R, Statmann RE, Yazyev O, Austin AJ, Cammi R, Pomelli C, Ochterski JW, Ayala PY, Morokuma K, Voth GA, Salvador P, Dannenberg JJ, Zakrzewski VG, Dapprich S, Daniels AD, Strain MC, Farkas O, Malick DK, Rabuck AD, Raghavachari K, Foresman JB, Ortiz JV, Cui Q, Baboul AG, Clifford S, Cioslowski J, Stefanov BB, Liu G, Liashenko A, Piskorz P, Komaromi I, Martin DJ, Fox T, Keith MA, Al-Laham CY, Peng A, Nanayakkara M, Challacombe RL, Gill PMW, Johnson B, Chen W, Wong MW, Gonzalez C, Pople JA. Gaussian Inc., Pittsburgh, PA, 2003.
21. Cheeseman JR, Frisch MJ, Delvin FJ, Stephens PJ. Ab initio calculation of atomic axial tensors and vibrational rotational strengths using density functional theory. Chem Phys Lett 1996;252:211–220.
22. Cappelli C, Corni S, Mennucci R, Cammi R, Tomasi J. Vibrational circular dichroism within the polarizable continuum model: a theoretical evidence of conformation effects and hydrogen bonding for (*S*)-(−)-3-Butyn-2-ol in CCl_4 Solution. J Phys Chem A 2002;106:12331–12339.
23. Seebach D, Beck AK, Dahinden R, Hoffmann M, Kuehnle FNM. Reduction of ketones with LiAlH4 complexes of a,a,a′,a′-tetraaryl-1,3-dioxolane-4,5-dimethanols (TADDOLs). A combination of enantioselective reduction and clathrate formation with a discussion of LAH reagents bearing C2-symmetrical ligands. Croat Chem Acta 1996;69:459–484.
24. Kirby AJ. The anomeric effect and related stereoelectronic effects at oxygen. Berlin: Springer-Verlag; 1983. p. 75